

Accepted Manuscript

FT-IR, FT-Raman, UV, NMR Spectra and Molecular Structure investigation of (E)-1-(3-chloropyrazin-2-yl)-2-(3-ethyl-2, 6-diphenyl piperidin-4-ylidene) hydrazine: A combined Experimental and Theoretical study

A. Therasa Alphonsa, C. Loganathan, S. Athavan, Dr. S. Kabilan



PII: S0022-2860(15)30135-6

DOI: [10.1016/j.molstruc.2015.07.024](https://doi.org/10.1016/j.molstruc.2015.07.024)

Reference: MOLSTR 21679

To appear in: *Journal of Molecular Structure*

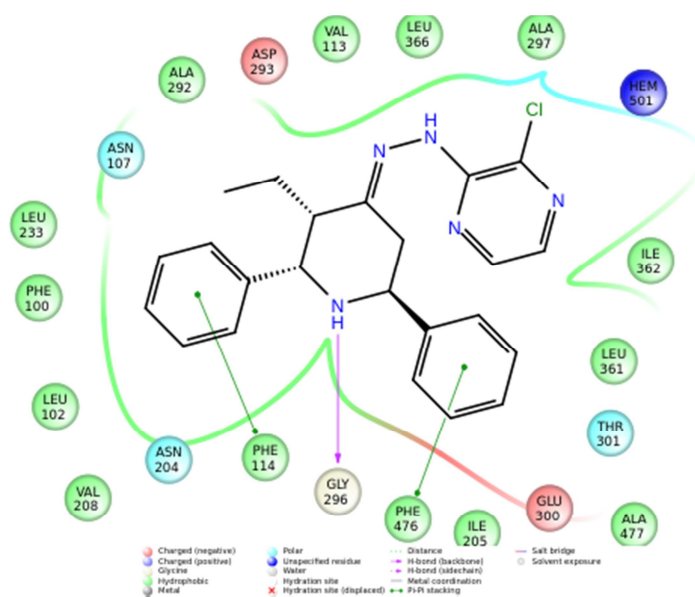
Received Date: 6 April 2015

Revised Date: 16 June 2015

Accepted Date: 13 July 2015

Please cite this article as: A. Therasa Alphonsa, C. Loganathan, S. Athavan, S. Kabilan, FT-IR, FT-Raman, UV, NMR Spectra and Molecular Structure investigation of (E)-1-(3-chloropyrazin-2-yl)-2-(3-ethyl-2, 6-diphenyl piperidin-4-ylidene) hydrazine: A combined Experimental and Theoretical study, *Journal of Molecular Structure* (2015), doi: 10.1016/j.molstruc.2015.07.024.

This is a PDF file of an unedited manuscript that has been accepted for publication. As a service to our customers we are providing this early version of the manuscript. The manuscript will undergo copyediting, typesetting, and review of the resulting proof before it is published in its final form. Please note that during the production process errors may be discovered which could affect the content, and all legal disclaimers that apply to the journal pertain.



FT-IR, FT-Raman, UV, NMR Spectra and Molecular Structure investigation of (E)-1-(3-chloropyrazin-2-yl)-2-(3-ethyl-2, 6-diphenyl piperidin-4-ylidene) hydrazine: A combined Experimental and Theoretical study

A. Therasa Alphonsa^a, C. Loganathan^a, S. Athavan^a, S. Kabilan^{a*}

^aDepartment of Chemistry, Annamalai University, Annamalainagar - 608002, Tamilnadu, India.

Abstract

This work presents the characterization of (E)-1-(3-chloropyrazin-2-yl)-2-(3-ethyl-2, 6-diphenyl piperidin-4-ylidene) hydrazine (HDE) by quantum chemical calculations and spectral techniques. The structure was investigated by FT-IR, FT-Raman, UV-Vis and NMR techniques. The geometrical parameters and energies have been obtained from Density functional theory (DFT) B3LYP (6-31G (d, p)) basis set calculations. The geometry of the molecule was fully optimized, vibrational spectra were calculated and fundamental vibrations were assigned on the basis of total energy distribution (TED) of the vibrational modes, calculated with scaled quantum mechanics (SQM) method. ¹H and ¹³C NMR chemical shifts of the molecule were calculated using Gauge-independent atomic orbital method (GIAO). The electronic properties such as excitation energies, wavelength, HOMO, LUMO energies performed by Time dependent density functional theory (TD-DFT) results complements with the experimental findings. NBO analysis has been performed for analyzing charge delocalization throughout the molecule. The calculation results were applied to simulate spectra of the title compound, which show excellent agreement with observed spectra. To provide information about the interactions between human cytochrome protein and the novel compound theoretically, docking studies were carried out using Schrödinger software.

*Corresponding author: Dr. S. Kabilan

Email: profdrskabilanaa@gmail.com, Tel: 9443924629

Keyword: TED, Docking, HOMO, LUMO, NBO and Hyperpolarizability.

1. Introduction

In recent years there has been a growing interest pertaining to the synthesis of heterocyclic systems owing to their varied reactivity, biological and physiological activity [1-5]. Nitrogen containing heterocycles always signified a subject of great interest due to their ubiquity in nature and massive presence as part of the skeletal backbone of many therapeutic agents. Piperidones have an important role in the field of medicinal chemistry due to their biological activities, including anticancer and cytotoxic properties [6]. Piperidones are also reported to possess analgesic, anti-inflammatory, central nervous system (CNS) stimulating, local anesthetic, anticancer and antimicrobial activity [7]. Particularly due to their varied biological properties such as antiviral, antifungal [8] and anti tumor analgesic [9] activities, 4-piperidones gaining a considerable importance. Also it plays an important role which embraces the organometallic field in different aspects [10-13].

Prostakov and Gaivoronskaya have reviewed about the significance of piperidin-4-one as intermediate in the synthesis of compounds of physiologically active [14]. The extensive studies undertaken in the past on 4-piperidones have their relation to the synthesis of drug [15]. Noller & Baliah prepared substituted piperidones by heating a mixture of ketone, aldehyde and ammonium acetate in acetic acid in the ratio of 1:2:1 [16]. Introduction of various substituents on the piperidone heterocycle improved the biological efficiency. When 2- and/or 6-positions of 4-piperidones are occupied by aryl groups, their biological activities are improved. The presence of alkyl substitution in 2 or 3 position is also attributed to biological activities [17-18]. A series of 2, 6-diphenyl-4-piperidone are

synthesized by different dialkyl ketone, aromatic aldehyde and ammonium acetate by Mannich condensation reaction [16].

Literature survey reveals that to the best of our knowledge, inadequate experimental and theoretical studies have been made on the vibrational, absorption spectra of piperidone and its derivatives. Most recently Paulo R. Oliveto et al investigated the spectroscopic and theoretical studies of 3-(4' substituted phenyl sulfanyl)-1-methyl-2-piperidone [19]. Subashchandrabose et al analyzed the spectroscopic FT-IR, FT-Raman and energy distribution of 3-pentyl-2, 6-diphenyl piperidin-4-one [20]. In addition to these studies, number researches are also done about the antimicrobial activities of piperidone derivatives [21-23]. To the best of our knowledge, neither experimental nor theoretical studies of the title compound have not been available until now.

In our present work, the molecular structural parameters like bond length, bond angle, dihedral angle, electronic, translational, rotational and vibrational frequencies, NBO have been calculated for the compound, (E)-1-(3-chloropyrazin-2-yl)-2-(3-ethyl-2,6-diphenyl piperidin-4-ylidene) hydrazine (HDE) (Fig.1). Optimized structural parameters are obtained using the Density Functional Theory (DFT), performing B3LYP/ (6-31G, d, p) level of calculations. The calculated molecular structural parameters and vibrational frequencies have been analyzed and compared with the experimental values. HOMO, LUMO analysis with UV spectroscopic studies is used to elucidate the information about the charge transfer within the molecule.

2. Experimental

2.1. Synthesis

2, 3-dichloro pyrazine, ammonium acetate, Benzaldehyde, 2-pentanone are purchased from Sigma-Aldrich chemical company with a stated purity and are used as such without further purification. The title compound is synthesized according to scheme 1.

2.2. Instruments

The FT-IR spectrum of the molecule is recorded in the region of 400- 4000 cm^{-1} on Thermo Scientific Nicolet iS5 (iD1 transmission) using KBr pellet. FT-Raman spectrum is recorded using 1064 nm line of Nd: YAG laser as excitation source with wave length in the region 3500-50 cm^{-1} on a Bruker RFS 100/S FT-Raman spectrophotometer. The detector is a liquefied nitrogen cooled Ge detector. The Ultraviolet absorption spectra of HDE dissolved in DMSO are examined in the range of 200 -800 nm using a Hitachi model U-2001 spectrophotometer. NMR spectrum is performed in Bruker DPX 400 MHz at 300K. The compound is dissolved in DMSO-d₆. Chemical shifts are reported in ppm relative to tetramethylsilane (TMS) for protons and carbons. ¹H and ¹³C NMR spectra are obtained at a base frequency of 400 MHz and 100 MHz respectively.

2.3. Computational Techniques

All computational studies are carried out at Density Functional theory (DFT) level on a Dell workstation equipped with V3 quadcore, Xeon processor E3-1240, 3.40 GHz personal computer with 8 GB total RAM using Gaussian 09W program package [24]. DFT calculations are less time consuming and include a significant part of the electron correlation leading to good accuracy. The calculations are carried out with the Becke's three parameter exchange functional with the LYP correction (B3LYP) and the basis set, 6-31 G (d, p) are used in appropriate calculations. The computational work has begun with the conformational analysis of the compound. The selected geometric parameters of the optimized structure of HDE are given in Table 1S.

2.4. Docking Studies

The Docking studies reported in this work were performed on a Dell workstation equipped with V2 quadcore, Xeon processor E3-1225, 3.20 GHz personal computer with 8 GB total RAM and with Schrödinger software suite, LLC, New York, 2012.

Molecular Docking study was performed by P450 2C19 proteins (human cytochrome P450 monooxygenase) to find the binding and interaction properties of synthesized compounds. The 3D crystallographic structure of human cytochrome protein complex [25] (PDB ID: 4GQS) was downloaded from Protein Data Bank (www.rcsb.com). The protein complex was prepared after pre-processing by Protein Preparation Wizard [26] in Maestro 9.3.5 version of Schrödinger software. The minimization of the protein complex was continued using OPLS-2005 (Optimized Potential for Liquid Simulations) force field [27] until the root mean square deviation (RMSD) reached the value of 0.3 Å.

The 2D structure of compound HDE was imported from the project table and the structure was minimized and geometrically refined using Ligprep [28] module. Conformers were generated using OPLS-2005 force field and torsional search method with distance dependent dielectric solvation treatment. The extra precision (XP) mode of docking was used to find the interactions between the active site of human cytochrome protein and the synthesized molecule using Glide [29] application of the Schrödinger software suite.

3. Results and Discussion

3.1. Vibrational analysis

The synthesized HDE is subjected to IR and Raman spectral analysis and the observed IR and Raman spectrum of HDE is given in Figure 1S. The theoretical vibrational spectra of the compound HDE are analyzed using DFT/B3LYP 6-31G (d, p) Table 2S. The non-negative vibrational frequency obtained from DFT calculations confirms that the optimized geometry of compound HDE is located at the minima on the potential energy state.

The theoretical vibrational frequencies are found to be in good agreement with the observed vibrational frequencies. The theoretical vibrational frequencies obtained for compound HDE is interpreted by means of Total energy distribution (TED %) calculations using SQM method. The normal modes assignment of the theoretical IR frequencies is visualized and substantiated with the help of the Gaussview 5.0 visualization program. The synthesized HDE consists of 53 atoms and hence has 162 normal modes of vibrations which includes 115 stretching, 116 bending and 93 torsional modes of vibration. Scaling factor values[30]of 0.96 used for C-H,C-X stretching, bending,wagging,ring puckering and torsion vibrational [31] frequencies, respectively. The molecule HDE belongs to C1 symmetry. The significant normal modes with TED (**10%**) are given in Table 2S.

N-H vibrations

The experimental wave number of 3414cm^{-1} in the IR and 3412cm^{-1} (mode no: 153) in the Raman spectrum of HDE is attributed for N-H stretching. The N-H stretching vibration modes are visualized in the mode nos.153 and 152 with the scaled frequencies 3433cm^{-1} to 3357cm^{-1} respectively. Both the obtained theoretical and vibrational frequencies are pure vibrations with TED % of 100 %.

Aromatic stretching group vibrations

In general, the aromatic C-H stretching frequencies appear in the range of $3100\text{-}3000\text{ cm}^{-1}$ [32] and the ring C-C stretching vibrations occur in the region $1650\text{-}1400\text{ cm}^{-1}$ [33]. In the present work, the bands observed at 3102 cm^{-1} and 3103 cm^{-1} in both infrared and Raman spectra for HDE have been assigned to the aromatic C-H stretching vibrations. In theoretical calculation, mode nos.140-151 corresponds to the theoretical aromatic C-H stretching vibrations.

Methyl, methylene group vibrations

The methyl groups present in HDE undergoes vibrations like symmetric stretching, asymmetric stretching, symmetric and asymmetric bending modes. The symmetric and asymmetric stretching mode of the methyl group appears in the range of 2860-2935 cm^{-1} and 2925-2985 cm^{-1} [34]. The stretching in the methyl groups is well explained by the mode nos. 112 and 110 in the theoretical vibrational study of the compound HDE. The theoretical wave numbers go well with the experimental both IR and Raman wave numbers. The bending vibrations of the methyl group are found to appear in the region of 1465-1440 cm^{-1} and 1390-1370 cm^{-1} [35]. The bending vibrations of the methyl groups are observed at 1411, 1412 cm^{-1} in the IR and Raman spectrum. The theoretical investigation well explains these bending vibrations as asymmetric bending vibration of the methyl group with the help of the mode no.112 in the scaled frequency of 1429 cm^{-1} .

The asymmetric and symmetric C-H stretching in methylene group normally appears in the region of 3100-2900 cm^{-1} [36]. In the present study, the observations of asymmetric and symmetric stretching of the C-H in methylene group (C7) in compound HDE observed at 2970, 2932 and 2934 cm^{-1} both in IR and Raman spectrum are complemented by the theoretical investigation which well explains the asymmetric and symmetric stretching in the methylene group in the respective scaled frequencies 3011, 2990, 2949, 2928, and 2908 cm^{-1} (mode nos.138, 136-134, 132). The bending vibration of the methylene group is explained theoretically in the frequency range 1457, 1452 cm^{-1} (mode no.120, 119). The bending vibration of the methylene group is observed at 1459 cm^{-1} .

C=N Vibrations

The C=N vibration normally appears in the region 1471 – 1689 cm^{-1} [37]. The strong band observed at 1719 cm^{-1} in the experimental IR spectra (1716 cm^{-1} in FT-Raman) of HDE

is assigned to C=N vibration. The mode no 129 with the scaled frequency 1647 cm^{-1} visualizes the C=N stretching.

N-N Vibrations

The experimental wave number of 949 cm^{-1} in the IR spectra whereas in Raman at 951 cm^{-1} of HDE is attributed for N-N stretching. The N-N stretching vibration mode is visualized in the mode no. 69 with the scaled frequency 948 cm^{-1} .

3.2. ^1H and ^{13}C NMR spectral analysis of HDE.

The ^1H NMR spectrum of HDE has been given in Figure 2S. In the ^1H NMR spectrum of the compound HDE Table 1 in which H (7) signal appears as triplet at δ 0.721 ppm. The multiplet at δ 1.290 ppm in the ^1H NMR indicates the presence of H (6). The H (3) protons are exposed in the region around δ 4.741 to 4.968 ppm. The doublet at δ 2.69 ppm in the ^1H NMR spectrum of the compound HDE shows the presence of H (8) protons. The ^1H NMR spectrum of HDE reveals a multiplet at δ 3.73 ppm for H (2) attached to a phenyl ring with the integral value corresponding to four protons.

The ^{13}C NMR spectrum of the compound HDE has been displayed in Figure 3S. The carbon chemical shifts are presented in Table 1. The ^{13}C NMR spectrum of the synthesized compound HDE has been recorded in DMSO. The low field signal observed around δ 10 ppm in ^{13}C NMR spectra of HDE is due to the carbon C (5). The C (8) carbon is identified at δ 63.0 ppm in ^{13}C NMR of HDE. The carbon in the azine linkage C (23) and C (4) are shielded by the electron cloud and hence exposed by the up-field signals in the range δ 158.1 ppm to δ 160.6 ppm. The signal at δ 59.2 ppm in the ^{13}C NMR spectrum of HDE is due to the carbon C (2).

The ^{13}C NMR peaks of the C5 carbon atom appear to be the same in experimental and theoretical values for which it is presented in the Table 1.

NMR spectroscopy is the key to reveal the conformational analysis of organic molecules. Good quality geometries must be taken into consideration for the quantum calculation of the absolute isotropic magnetic shielding tensors to yield more reliable results. There are many reports on NMR isotropic magnetic shielding tensor calculations employing the GIAO method associated with the Density functional theory (DFT) [38]. The GIAO ^1H NMR and ^{13}C NMR chemical shift calculations of the stable conformer is made in DMSO [scrf= (solvent=DMSO)] by using B3LYP / 6-31G (d, p) basis set. The isotropic values in the calculations are subtracted from a scaling factor of 182.4656 and 31.882 to obtain the chemical shifts for ^{13}C and ^1H NMR respectively. The obtained chemical shift values were compared with the experimentally observed values. The observed and the calculated carbon chemical shift values are found to be in good agreement whereas the theoretical ^1H NMR chemical shifts are found to be lesser than the experimental values. The calculated values are given in the Table 1 along with the observed values. The relationship between the experimental chemical shift and computed chemical shift values are given in Figure 2. The relation between the observed and computed values predicts that the conformation deduced theoretically should be the favorable conformation of the synthesized HDE.

3.3. Natural Bond orbital analysis

The natural bond orbital analysis provides an efficient method for studying intra-and intermolecular bonding and interaction among bonds, and also provides a convenient basis for investigating charge transfer or conjugative interaction in molecular systems, it could enhance the analysis of the delocalization of charge in the system.

The donor bonding orbitals, the acceptor antibonding orbitals, the donor lone pair atoms are given in Table 2 along with the $E(2)$ values which estimates the interaction between the donor (filled) and acceptor (vacant) orbitals. The $E(2)$ energy is the lowering energy that occurs during the hyperconjugative electron transfer process and hence $E(2)$ can

be referred to as stabilization energy. Larger the $E(2)$ values, greater is the stability of the molecule. In the NBO analysis of the compound HDE, the $E(2)$ values are greater for the delocalization of the electrons between the bonds present in the phenyl ring. The lone pair of electrons present in the Nitrogen atom N22 is delocalized to C3-N28 antibonding orbitals with high delocalization energy which may be attributed to the presence of chloro substituent. The delocalization of electrons from the lone pair of the Nitrogen atom N21 to C4 – C5 antibonding orbitals is not so effective because of the absence of electron withdrawing group in the rings nearer to N21.

3.4. Charge Analysis

The charge quantifies the electronic structure changes under atomic displacement. It is related directly to the chemical bonds present in the molecule, it influences dipole moment, polarizability, electronic structure and more properties of molecular systems. Natural charge analysis tends to predict larger charges than several other population analysis like Mulliken charges. Natural charges considers the population in the orbitals that will overlap to form a bond and those that are too near the core of an atom to be involved in bonding. Mulliken charges are the partial charges confined to the atoms. The Mulliken and natural charge distribution of the molecule calculated on B3LYP level with 6-31G (d, p) basis set are shown in Table 3. The Mulliken charge distribution in the compound HDE is found to be greater than the corresponding natural charges (Figure 3). The carbon atoms 4C, 23C and 24C possess positive charges in Mulliken charge and natural charge analysis. The carbon atoms 2C, 15C, 27C, 26C and 9C possess positive Mulliken charge and negative natural charge. All the hetero atoms in the compounds possess negative Mulliken and negative charges.

3.5. Molecular electrostatic potential (MEP) surfaces

The reactive behavior of the molecule is visualized with the help of three dimensional MEP surface. MEP surface describes the charge distribution in the molecule and helps in

predicting the sites for nucleophilic and electrophilic attack in the molecule. The MEP surface has been plotted for the molecules HDE in Figure 4. Region of negative charge is pictured out in red colour and it is found around the electronegative Cl and N in the azine linkage in the molecule HDE. The red colour region is susceptible to electrophilic attack. The blue colour region represents strong positive region and is prone to nucleophilic attack. The green colour region corresponds to a potential half way between the two extremes red and blue region.

3.6. HOMO-LUMO Pictures of HDE

HOMO-LUMO pictures of molecule HDE is presented in Figure 5. The p_z Orbitals of C15,C16,C17,C18,C19,C20,C7,C9,C10,C11,C12,C13 and C14 carbon atoms do not involve in the formation of the HOMO orbitals in the molecule HDE. The p_z orbitals of C6,C7,N1,C5,C8 C9,C10,C11,C12,C13,C14,C20,C15,C16,C17,C18,C19 and C20 carbon atoms alone do not involve in the formation of the LUMO orbital. The band gap between the HOMO and LUMO orbital energy is found to be 4.485 eV.

3.7. Polarizability calculations of HDE

The calculated values of the dipole moment (μ), the polarizability (α_0) and first hyperpolarizability (β_{tot}) by finite field approach are given in Table 4 along with the corresponding components. The field independent and field dependent dipole moment μ values of are calculated to be 2.71 and 0.78 respectively. The highest value of dipole moment is observed for the component μ_y for both the field independent and dependent conditions. The compound HDE is found to be a polar molecule having non – zero dipole moment components.

The calculated polarizabilities α_{ij} have non – zero and are dominated by the diagonal components. The β_{tot} value of HDE is found to 3.212×10^{-30} esu. Delocalization of charges in particular directions is indicated by large values of those particular components of

polarizability and hyperpolarizability, first order hyperpolarizability is dominated by β_{xzz} and β_{zzz} values. This shows that the delocalization of the charges in the presence of an external field is endorsed in those directions. The first hyperpolarizability of HDE ($\langle\beta\rangle_{\text{tot}}$) is 9 times greater than that of urea (0.3728×10^{-30} esu), hence this molecule can have a considerable NLO activity and can find its application in the material science field too.

3.8. UV spectrum and electronic properties

The UV absorption spectrum of the title compound in DMSO solvent was recorded within the 200-400 nm range and representative spectrum is shown in Figure 4S. It is observed that the recorded absorption bands centered at 278 nm in DMSO. In order to support our experimental observations TD-DFT calculations on electronic absorption spectra were performed based on the B3LYP/6-31G (d, p) [39] level optimized structure in gas phase. The TD-DFT method predicted the maximum absorption peak at 272 nm with strong oscillator strength, while this peak was recorded at 278 nm in DMSO. Due to the Frank-Condon principle this peak (λ_{max}) corresponds to vertical excitation. Calculations of the molecular orbital geometry show that the visible absorption maxima of this molecule correspond to the electron transition between frontier orbitals such as transition from HOMO to LUMO. The HOMO energy characterizes the ability of electron giving, the LUMO characterizes the ability of electron accepting, and the gap between HOMO and LUMO characterizes the molecular chemical stability [40]. The energy gap between the HOMOs and LUMOs is a critical parameter in determining molecular electrical transport properties because it is a measure of electron conductivity. The absorption maximum values are observed at 278 nm, those show agreement with theoretical values. The deviation between experiment and theory may be resulted from solvent effects. Solvent makes the chemical environment of the molecule in the simulation become very complex. The maximum absorption wavelength corresponds to the electronic transition from the highest occupied molecular orbital HOMO to lowest

unoccupied molecular orbital LUMO. All the observed transitions are π - π^* ones. All assignments agree well with the values available in the literature and experimental values.

3.9. Docking studies

Docking studies were carried out to evaluate the binding affinity and the interactions between the synthesized compound and the human cytochrome protein (PDB ID: 4GQS). The docking score of the different conformers of compound HDE varies from -8.4 to -3.6. The docking results clearly indicate that the tested compound display two types of interactions with three amino acids present in the active site of 4GQS. The 2D and 3D view of interactions between the compound and 4GQS is shown in Figure 6. The aromatic rings present in the 2nd and the 6th positions of the piperidyl ring were showed π - π stacking interactions with PHE114 and PHE476 residues. The $-NH$ group of the piperidyl ring shows hydrogen bond interaction with GLY296 residue.

4. Conclusions

A novel Unsymmetrical azine (E)-1-(3-chloropyrazin-2-yl)-2-(3-ethyl-2,6-diphenyl piperidin-4-ylidene) hydrazine (HDE) was synthesized and characterized by FT-IR, FT-Raman, UV-Vis, 1H and ^{13}C techniques. The theoretical IR vibrational frequencies are found to be in good agreement with the observed and theoretical IR vibrational frequencies of HDE are analyzed by means of total energy distribution (TED%) calculations using scaled quantum mechanics (SQM) method. The GIAO 1H and ^{13}C NMR chemical shift calculations of the stable conformer is made in DMSO by using B3LYP/6-31G (d,p) basis set. The compound HDE is subjected to NBO analysis, the E(2) values are greater for the delocalization of the electrons between the bonds present in the phenyl ring. In the Nitrogen atom N22 antibonding orbitals with high delocalization energy which may be due to the presence of chloro substituent. The first hyper polarizability of HDE is 9 times greater than of urea (0.3728×10^{-30} esu), hence this molecule can have considerable NLO activity and can

find its application in material science field too. The docking results clearly indicate that the tested compound display two types of interactions with three amino acids present in the active site of 4GQS.

References:

- [1] P.M. Weintraub, J.S. Sabol, J.M. Kane and D.R. Borchering, *Tetrahedron* 59 (2003) 2953-2989.
- [2] G.L. Arutyunyan, A.A. Chachoyan, V.A. Shkulev, G.G. Adamyan, T.E. Agadzhanyan and B.T. Garibdzhanyan, *Khim. Farm. Zh.* 29 (1995) 3335.
- [3] C. Jobin, C.A. Bradham, M.P. Russo, B. Juma, A.S. Narula, D.A. Brenner and R.B. Sartor, *J. Immunol.* 163 (1999) 3474-3483.
- [4] C.R. Ganellin and R.G. Spickett, *J. Med. Chem.* 8 (1965) 619-625.
- [5] B. Ileana, V. Dobre and I. Niculescu-Duvaz, *J. Prakt. Chem.* 327 (1985) 667-674.
- [6] J.R. Dimmock, et al., *Drug design and delivery* 6 (1990) 183-194.
- [7] R.V. Perumal, M. Adiraj and P. Shanmugapandiyam, *Indian Drugs* 38 (2001) 156-159.
- [8] P. Parthiban, G. Aridoss, P. Rathika, V. Ramkumar, S. Kabilan, *Bioorg. med. Chem. Lett.* 19 (2009) 6981-6985.
- [9] G. Aridoss, P. Parthiban, R. Ramachandran, M. Prakash, S. Kabilan, T. Jeongy, *Eur. J. Med. chem.* 44 (2009) 577-592.
- [10] H.M. Garrafo, J. Caceres, J.W. Daly, T.F. Spande, N.R. Andriamaharavo and M. Andriantsiferana, *J. Nat. Prod.* 56 (1993) 1016-1038.
- [11] S.R. Angle, J.G. Breitenbucher, *Studies in Natural Products Chemistry* Elsevier 16 (1995) 453-502.
- [12] V. Padmavathi, T.V. Ramana Reddy, K. Audishesha Reddy, A. Padmaja and A. Bhaskar Reddy, *Indian. J. Chem.* 44B (2005) 2527-2531.
- [13] A.R. Kartritzky and W.Q. Fan, *J. Org. Chem.* 55 (1990) 3205-3209.
- [14] N. S. Prostakov, L. A. Gaivoronskaya, *γ -Piperidinones in Organic Synthesis*, *Chem. Rev.* 47 (1978) 447-469.
- [15] D. Lednecr, L. A. Mitcher, John Wiley & sons, New York, (1977); A. Burger, *Medicinal Chemistry, Part II*, Wiley Inter Science, New York, (1970) 1609; T. N. Riley, D.B. Hale and M. C. Wilson *J. Pharm. Chem.* 62 (1973) 983-986.
- [16] C.R. Noller, V. Baliah, *J. Am. Chem. Soc.* 70 (1948) 3853-3855.

- [17] I.G. Mobio, A.T. Soldatenkov, V.O. Federov, E.A. Ageev, N.D. Sergeeva, S. Lin, E.E. Stashenko, N.S. Prostakov, E.I. Andreeva, *Khim. Farm. Zh.* 23 (1989) 421-427.
- [18] M. Nikolov, D. Stefanora, D. Chardanon, *Acta Nerv. Super.* 16 (1974) 264-267.
- [19] R. Paulo, Oliveto et al, *Molecules* 18 (2013) 7492-7509.
- [20] S Subashchandrabose, H. Saleem, Y. Erdogdu, G. Rajarajan, V. Thanikachalam, *Spectrochimica Acta Part A* 82 (2011) 260-269.
- [21] A. Senthil, P. Suresh Kumar, C.H. Narasimha Raju, S. Mohideen, S. Navaneetha Krishnan, *International Journal of Preclinical and Pharmaceutical Research* 2 (2011) 22- 25.
- [22] P. Pandey and P. Chawla, *International Journal of Pharmaceutical, Chemical and Biological Sciences* 2 (2012) 305-309.
- [23] N. Jayalakshmi and S. Nanjundan, *Int.J. Chem. Sci.* 6 (2008) 1177-1188.
- [24] R. J. Xavier, E. Gobinath, *Spectrochimica Acta Part A* 86 (2012) 242-251.
- [25] R. L. Reynald, S.Sansen, C. D. Stout and E. F. Johnson, *J. Biol. Chem.* 287 (2012) 44581- 44591.
- [26] Protein Preparation Wizard, Epic version 2.3, 2012, Schrödinger, LLC, New York, Impace version 5.7, 2012.
- [27] W. L. Jorgensen, D. S. Maxwell and J. Tirado-Rives, *J. Am. Chem. Soc.* 118 (1996) 11225–11236.
- [28] Schrödinger, Lig Prep, LLC, New York, , version 2.5, 2012,
- [29] Schrödinger, LLC, New York, Glide, version 5.8, 2012.
-

- [30] G. Rauhut, P. Pulay, *J. Phys. Chem.* 99 (1995) 3093.
-
- [31] A. P. Scott, L. Radom, *J. Phys. Chem.* 100 (1996) 16502.
- [32] Y. Li, Y. Liu, H. Wang, X. Xiong, P. Wei, F. Li, *Molecules* 18 (2013) 877-893.
- [33] H.T. Flakus, A. Miros, P. G.Jones, *Spectrochimica Acta Part A* 86 (2012) 242-251.
- [34] W.B. Tzeng, K. Narayanan, J.L.Lin, C.C.Tung, *Spectrochimica Acta Part A* 55 (1999) 53- 162.
- [35] H.K. Jeong, H.J. Noh, J.Y. Kim, M.H. Jin, C.Y. Park and Y.H. Lee, *Euro physics letters* 82 (2008) 67004.
-
- [36] S. Higuchi, E. Kuno, S.Tanaka and H. Kamada, *Spectrochimica Acta Part A* 28 (1972) 1335-1346.
- [37] R. Lu, W. Gan, B. Wu, Z. Zhang, Y. Guo and H. Wang, *J.phys.chem.B* 109 (2005) 14118- 14129.
- [38] L.J. Bellamy, *The infra red spectra of complex molecules*, second edition, Chapman and hall, London and New York, 1979.
- [39] P. Vijaya and K.R. Sankaran, *Spectrochimica Acta Part A* 138 (2015) 460-473.
- [40] N. Sundaraganesan, C. Meganathan, H.Saleem, B.D. Joshua, *Spectrochimica Acta Part A* 68 (2010) 259-269.
- [41] K. Fukui, *Science.* 218 (1982) 747–754.
-

FIGURE and SCHEME CAPTIONS

Scheme 1.

Fig. 1. Numbering of HDE used in this study

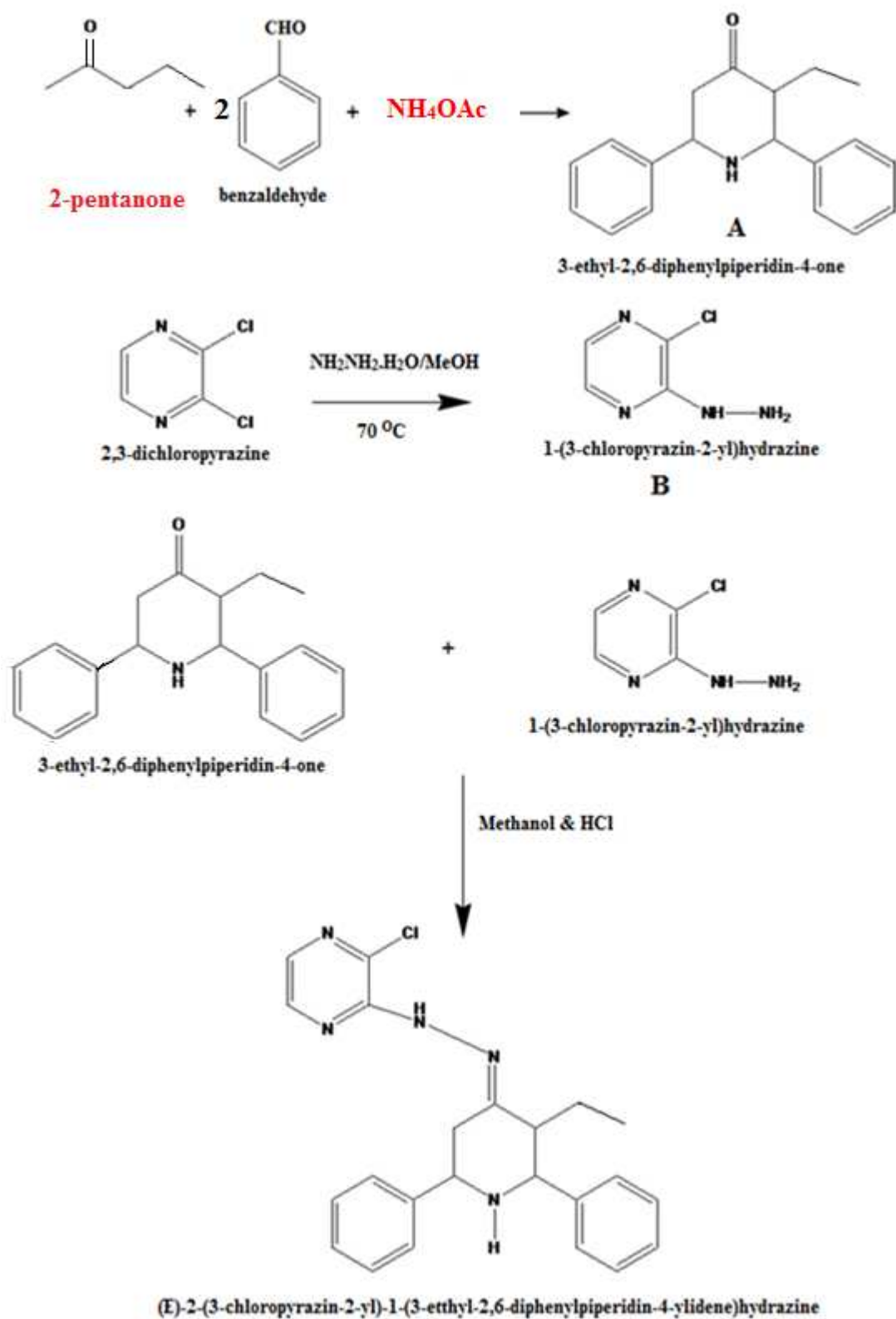
Fig. 2. Comparison of observed and theoretical chemical shifts values of ^1H and ^{13}C spectrum of HDE

Fig.3. Comparison of Mulliken charges and NBO charges of HDE

Fig. 4. MEP plot of HDE

Fig. 5. HOMO-LUMO pictures of HDE

Fig. 6. 2D and 3D interaction between HDE and 4GQS



Scheme 1

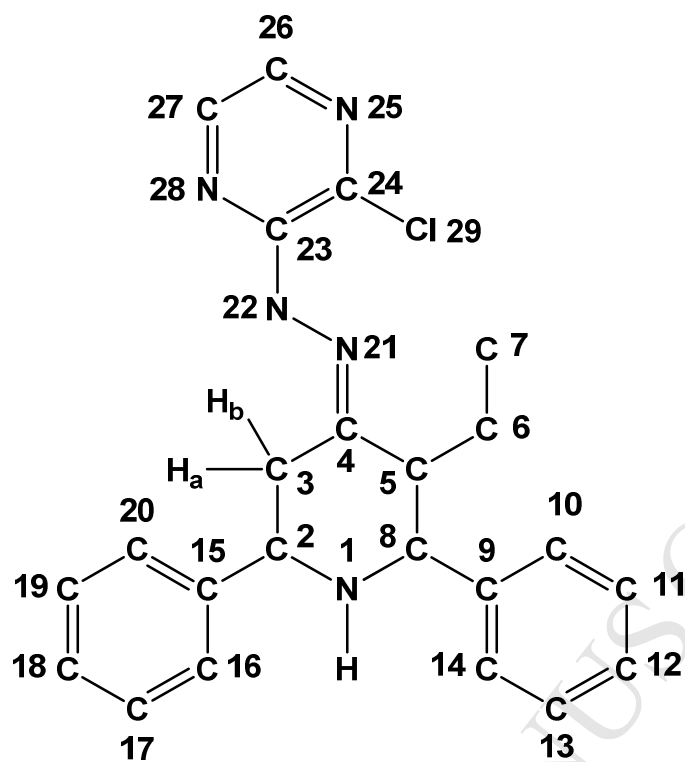


Fig. 1. Numbering of HDE used in this study

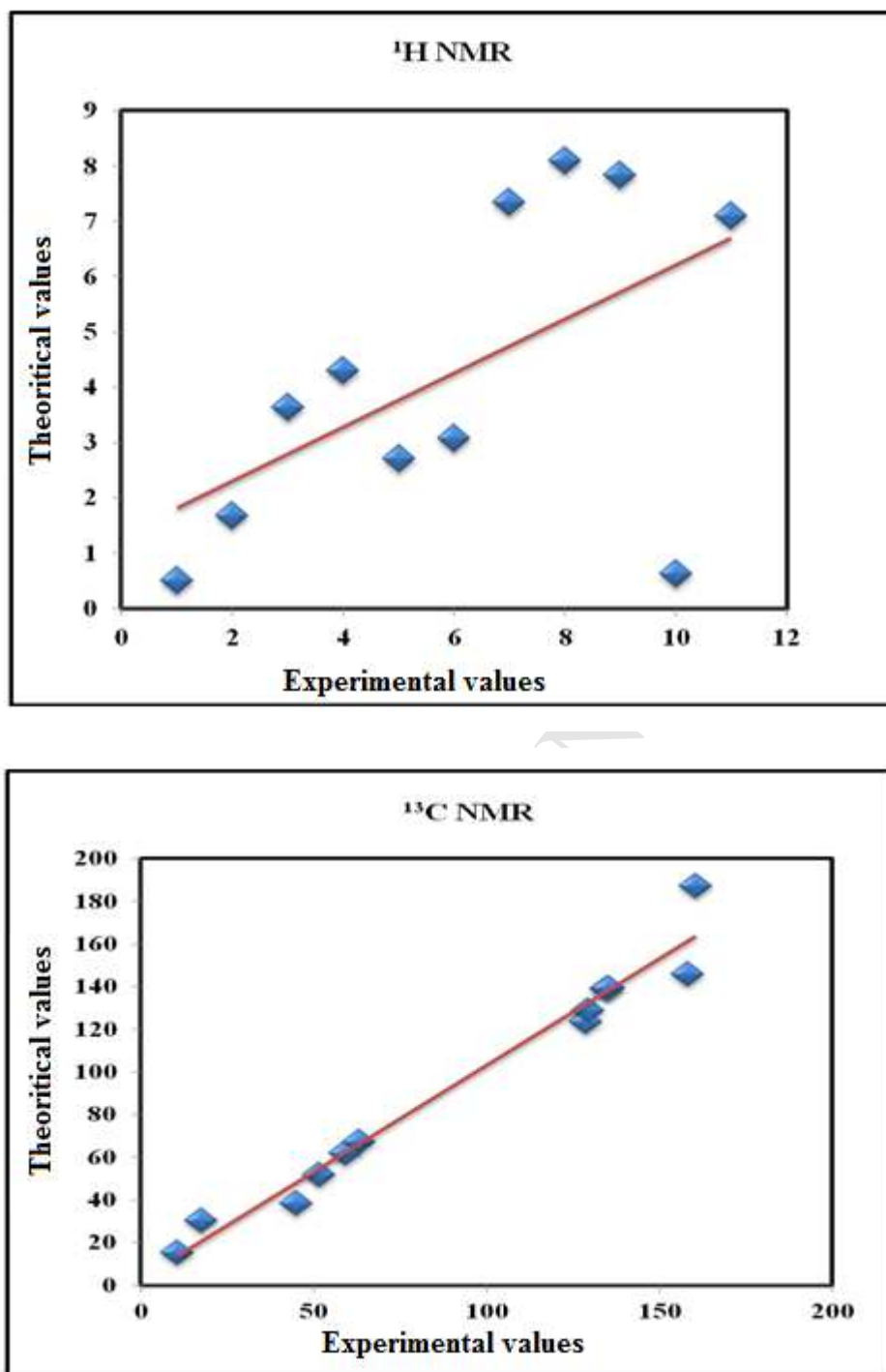


Fig. 2. Comparison of Experimental and theoretical chemical shifts values of ^1H and ^{13}C spectrum of HDE

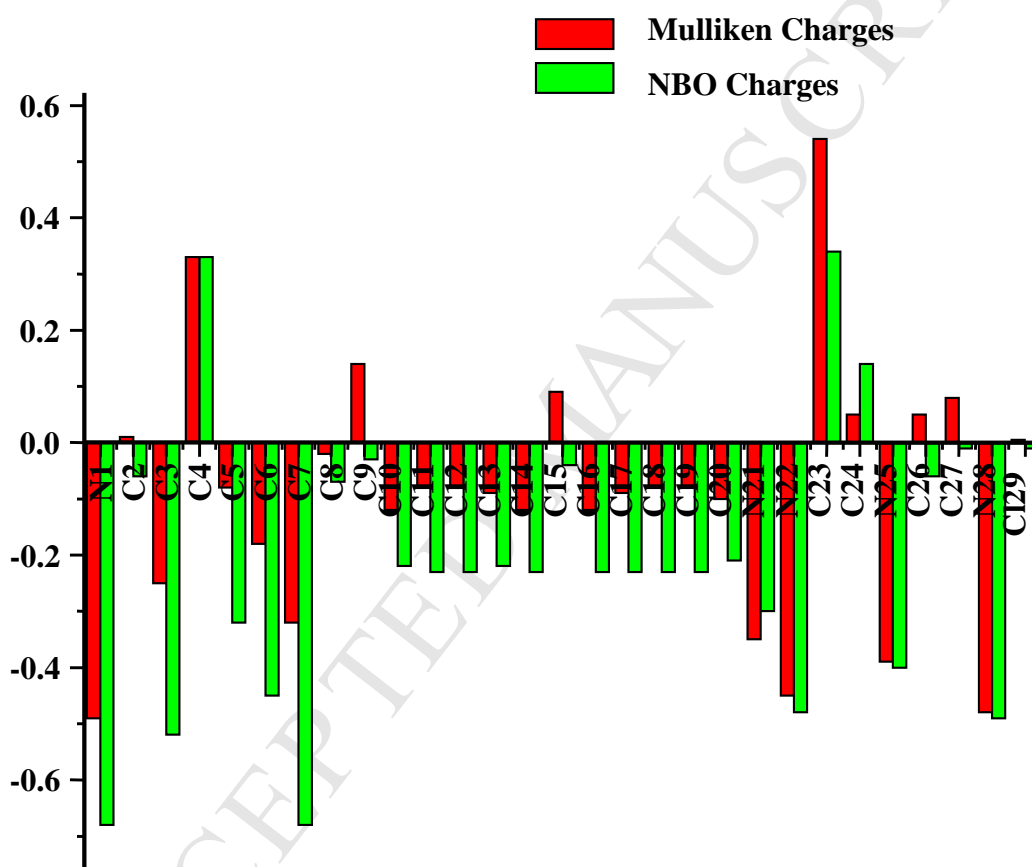


Fig. 3. Comparison of Mulliken charges and NBO charges of HDE

-4.978e-2  4.978e-2

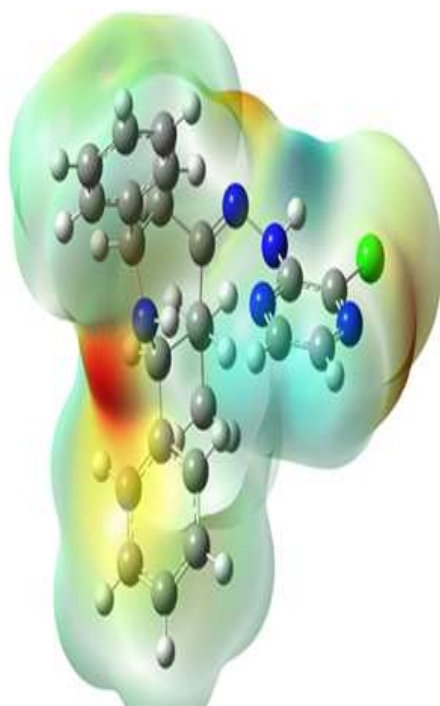
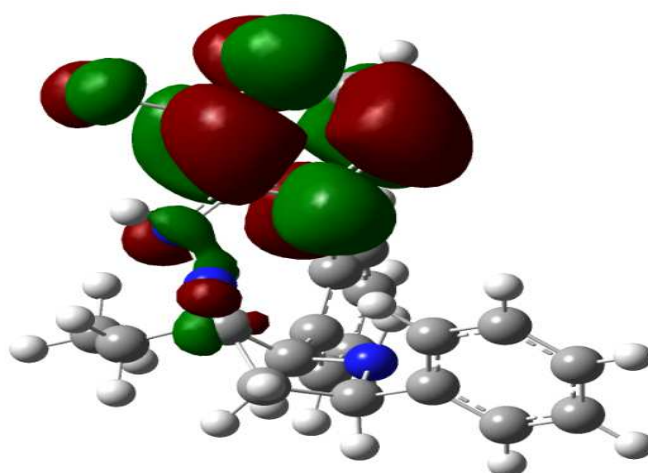
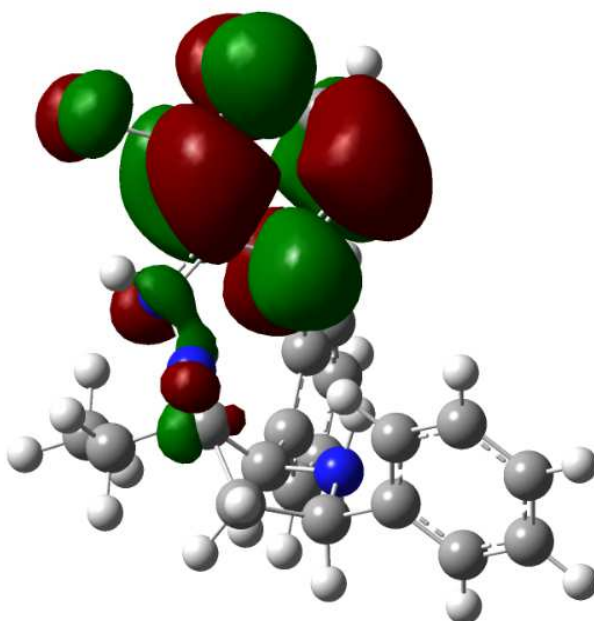


Fig. 4. MEP plot of HDE

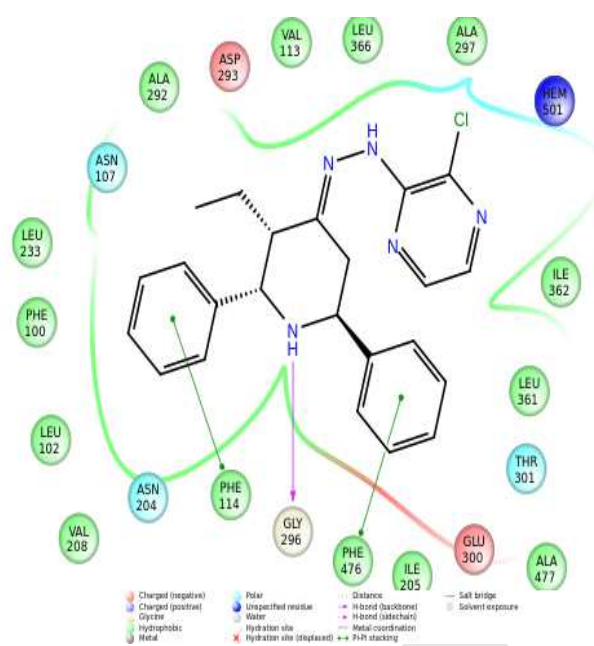


LUMO

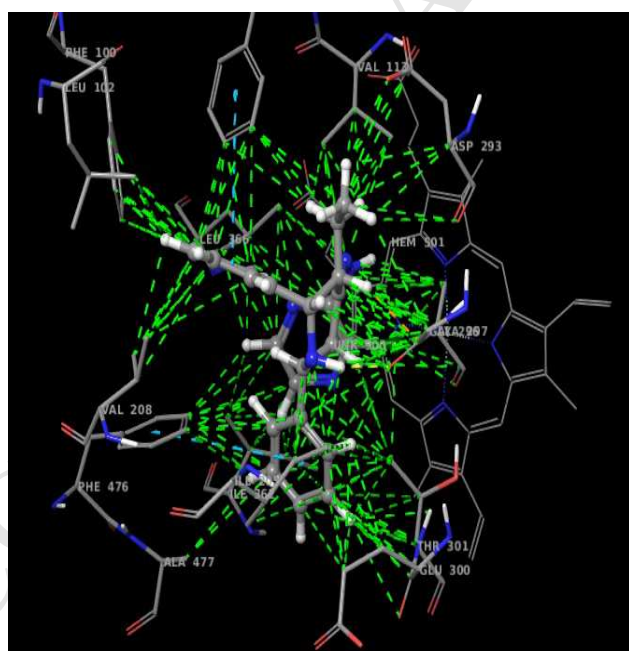


HOMO

Fig. 5. HOMO-LUMO pictures of HDE



2D view



3D view

Fig. 6. 2D and 3D interaction between HDE and 4GQS

TABLE CAPTIONS

Table 1. Experimental and computational ^1H and ^{13}C NMR spectral analysis of HDE in DMSO solution by DFT method

Table 2. Second order perturbation theory analysis of fock matrix in NBO basis for HDE

Table 3. Mulliken charges and NBO charges of HDE

Table 4. Dipole moment μ (D), mean polarizability α_0 ($\times 10^{-24}$ esu) and first hyperpolarizability β_{tot} ($\times 10^{-33}$ esu) of HDE by DFT method

Table 1. Experimental and computational ^1H and ^{13}C NMR spectral analysis of HDE in DMSO solution by DFT method ^1H chemical shift values

Atom	Expt.value	Theo.value
H7	0.721(t)	0.501
H6	1.290(m)	1.678
H8	2.695(d)	3.633
H2	3.737(m)	4.295
H3a	4.968(t)	2.705
H3b	4.741(t)	3.081
Aromatic protons	7.439(s)	7.342-7.698
H27	7.894(s)	8.102
H26	7.821(s)	7.839
H1--N1	10.046(s)	0.633
H22--N22	11.056(s)	7.105

 ^{13}C chemical shift values

Atom	Expt.value	Theo.value
C7	10.61	15.20
C6	17.44	30.15
C3	44.96	38.53
C5	51.68	51.64
C2	59.25	61.76
C8	63.03	67.32
Aromatic carbons	128.54	123.54
Pyrazine	129.28	128.91
Pyrazine	134.51	138.98
Pyrazine	135.44	139.41
Pyrazine	158.13	145.64
C4	160.61	187.31

Table 2. Second order perturbation theory analysis of fock matrix in NBO basis for HDE

Type	Donor (i)	ED (i,e)	Acceptor (j)	ED (j,e)	E2 (Kcal/Mol)	E(j)-E(i) a.u	F(i,j) a.u
π - π^*	C15-C16	1.65250	C20-C19	0.32736	20.15	0.28	0.067
π - π^*	C15-C16	1.65250	C17-C18	0.33339	20.75	0.28	0.068
π - π^*	C20-C19	1.66506	C15-C16	0.34552	20.55	0.28	0.068
π - π^*	C20-C19	1.66506	C17-C18	0.33339	20.35	0.28	0.068
π - π^*	C17-C18	1.66362	C15-C16	0.34552	20.02	0.28	0.068
π - π^*	C17-C18	1.66362	C20-C19	0.32736	20.24	0.28	0.068
π - π^*	C23-N28	1.70876	C24-N25	0.38584	14.26	0.30	0.060
π - π^*	C23-N28	1.70876	C27-C26	0.28739	25.49	0.33	0.082
π - π^*	C24-N25	1.79094	C23-N28	0.45173	15.82	0.32	0.068
π - π^*	C24-N25	1.79094	C27-C26	0.28739	16.43	0.35	0.069
π - π^*	C27-C26	1.66809	C23-N28	0.45173	15.04	0.26	0.058
π - π^*	C27-C26	1.66809	C24-N25	0.38584	22.04	0.26	0.068
π - π^*	C9-C14	1.64942	C10-C11	0.32914	19.57	0.28	0.066
π - π^*	C9-C14	1.64942	C13-C12	0.33364	21.30	0.28	0.069
π - π^*	C10-C11	1.66701	C9-C14	0.34568	20.85	0.29	0.069
π - π^*	C10-C11	1.66701	C13-C12	0.33364	20.03	0.28	0.067
π - π^*	C13-C12	1.66235	C9-C14	0.34568	19.64	0.29	0.067
π - π^*	C13-C12	1.66235	C10-C11	0.32914	20.58	0.28	0.068
σ - σ^*	N21	1.92884	C4-C5	0.04346	12.09	0.81	0.089
σ - π^*	N22	1.76998	C23-N28	0.45173	35.61	0.30	0.098
σ - σ^*	N28	1.90466	C23-C24	0.05890	10.75	0.84	0.086
σ - σ^*	N25	1.89411	C23-C24	0.05890	11.74	0.84	0.090
LP(3)- π^*	Cl29	1.92507	C24-N25	0.38584	13.81	0.31	0.063

a - energy of hyper conjugative interaction (stabilization energy), b - energy difference donor and acceptor i and j NBO orbitals, c - F (i-j) is the fock matrix element between i and j NBO orbitals

Table 3. Mulliken charges and NBO charges of HDE

Atom	Mulliken charges	NBO charges
N1	-0.49	-0.68
C2	0.01	-0.06
C3	-0.25	-0.52
C4	0.33	0.33
C5	-0.08	-0.32
C6	-0.18	-0.45
C7	-0.32	-0.68
C8	-0.02	-0.07
C9	0.14	-0.03
C10	-0.12	-0.22
C11	-0.08	-0.23
C12	-0.08	-0.23
C13	-0.09	-0.22
C14	-0.12	-0.23
C15	0.09	-0.04
C16	-0.12	-0.23
C17	-0.09	-0.23
C18	-0.08	-0.23
C19	-0.08	-0.23
C20	-0.10	-0.21
N21	-0.35	-0.30
N22	-0.45	-0.48
C23	0.54	0.34
C24	0.05	0.14
N25	-0.39	-0.40
C26	0.05	-0.06
C27	0.08	-0.01
N28	-0.48	-0.49
C129	0.005	-0.01

Table 4. Dipole moment μ (D), mean polarizability α_0 ($\times 10^{-24}$ esu) and first hyperpolarizability β_{tot} ($\times 10^{-33}$ esu) of HDE by DFT method

Parameters	Dipole moment	Parameters	First hyperpolarizability
μ_x	field independent	β_{xxx}	-56.26
	field dependent	β_{xxy}	351.79
μ_y	field independent	β_{xyy}	-497.59
	field dependent	β_{yyy}	-481.75
μ_z	field independent	β_{xxz}	-836.34
	field dependent	β_{xyz}	-191.29
μ	field independent	β_{yyz}	-129.46
	field dependent	β_{xzz}	1582.72
Parameters	Polarizability	β_{yzz}	98.62
α_{xx}	44.55	β_{zzz}	-2076.78
α_{xy}	-2.52	β_{tot}	3211.98
α_{yy}	40.79		
α_{xz}	-0.57		
α_{yz}	1.24		
α_{zz}	38.08		
α_0	41.14		

Highlights:

1. HDE is prepared and characterised by spectral studies.
2. Vibrational frequencies are computed and substantiated using TED%
3. NLO analysis predicts significant NLO activity of HDE.
4. From docking studies, the enhanced biological interaction of HDE is showcased.

SUPPLEMENTARY TABLES

Table 1S. Selected geometric parameters Bond length (Å), Bond angle (°) and Dihedral angle (°) of HDE computed by DFT method (B3LYP/6-31 G (d, p))

Table 2S. Experimental and theoretical wave numbers obtained for (FT-IR and Raman) spectral values of HDE

Figure 1S. Experimental Raman spectrum of HDE.

Experimental IR spectrum of HDE.

Figure 2S. Experimental ^1H NMR spectrum of HDE.

Figure 3S. Experimental ^{13}C NMR spectrum of HDE.

Figure 4S. UV spectrum of HDE.

Table 1S. Selected geometric parameters Bond length (Å), Bond angle (°) and Dihedral angle (°) of HDE computed by DFT method (B3LYP/6-31 G (d, p))

Parameters	Bond length (Å)	Parameters	Bond length (Å)
C4-C3	1.504	N22-H22	1.013
C4-C5	1.517	N22-C23	1.377
C4-N21	1.283	C23-C24	1.427
C3-C2	1.572	C23-N28	1.338
C2-N1	1.475	C24-N25	1.302
C2-C15	1.520	C24-C129	1.769
C8-C5	1.569	N28-C27	1.342
C8-N1	1.474	N25-C26	1.348
C8-C9	1.522	C27-C26	1.385
C5-C6	1.551	C6-C7	1.532
N1-H1	1.019	H7-C9	3.431
C15-C20	1.400	C9-C10	1.400
C15-C16	1.402	C9-C14	1.401
C20-C19	1.394	C10-C11	1.394
C16-C17	1.396	C14-C13	1.395
C19-C18	1.395	C11-C12	1.395
C17-C18	1.395	C13-C12	1.395
N21-N22	1.435		
Parameters	Bond angle (°)	Parameters	Bond angle (°)
C3-C4-C5	115.4	N21-N22-C23	118.3
C3-C4-N21	116.5	N22-C23-C24	121.3
C5-C4-N21	127.9	N22-C23-N28	119.7
C4-C3-C2	109.9	C24-C23-N28	118.7
C3-C2-N1	112.4	C23-C24-N25	123.2

C3-C2-C15	114.0	C23-C24-C129	119.0
N1-C2-C15	109.1	N25-C24-C129	117.62
C5-C8-N1	112.4	C23-N28-C27	117.66
C5-C8-C9	114.1	C24-N25-C26	117.4
N1-C8-C9	108.9	N28-C27-C26	122.4
C4-C5-C8	108.73	N25-C26-C27	120.3
C4-C5-C6	108.74	C5-C6-C7	114.6
C8-C5-C6	114.1	C8-C9-C10	119.9
C2-N1-C8	112.7	C8-C9-C14	121.6
C2-C15-C20	119.3	C9-C10-C14	118.3
C2-C15-C16	121.9	C43-C44-C46	121.0
C20-C15-C16	118.6	C43-C45-C48	120.7
C15-C20-C19	120.9	C44-C46-C50	120.0
C15-C16-C17	120.4	C45-C48-C50	120.2
C20-C19-C18	120.0	C1-N23-N24	184.4
C16-C17-C18	120.3	C1-N23-N24	4.7753
C19-C18-C17	119.5		
Parameters	Dihedral angle (°)	Parameters	Dihedral angle (°)
C5-C4-C3-C2	59.742	C9-C10-C11-C12	0.393
N23-C4-C3-C2	-119.8713	H47-C10-C11-C12	-179.4646
C3-C4-C5-C8	-34.443	C9-C14-C13-C12	0.1732
C3-C4-C5-C6	90.4135	C10-C11-C12-C13	0.1208
N21-C4-C5-C8	145.1185	C14-C13-C12-C11	-0.4006
N21-C4-C5-C6	-90.0251	C5-C8-C9-C14	51.1196
C3-C2-N1-C8	-38.0353	N1-C8-C9-C10	101.5413
C15-C2-N1-C8	-165.6155	N1-C8-C9-C14	-75.5292
C3-C2-C15-C20	141.973	C4-C5-C6-C7	172.9367
C3-C2-C15-C16	-40.3895	C8-C5-C6-C7	-65.4668
C9-C8-C5-C4	-151.1075	C2-C15-C20-C19	178.1793
C3-C4-N22-C23	99.8576	N22-C23-C24-N25	-178.2154
C5-C4-N22-C23	-77.0287	N22-C23-C24-C129	1.9886

C4-C3-C2-N1	-21.0753	C2-C15-C16-C17	-178.0913
C4-C3-C2-C15	103.8881	C20-C15-C16-C17	-0.4386
N1-C2-C15-C20	-91.3072	C15-C20-C19-C18	-0.1829
N1-C2-C15-C16	86.3303	C15-C16-C17-C18	0.133
N1-C8-C5-C4	-26.3335	C20-C19-C18-C17	-0.1316
N1-C8-C5-C6	-147.9376	C16-C17-C18-C19	0.156
C16-C15-C20-C19	0.4647	N21-N22-C23-C24	-151.7427
C9-C8-C5-C36	87.2884	N21-N22-C23-N28	30.4982
C5-C8-N1-C2	64.9575	C14-C9-C10-C11	-0.6122
C9-C8-N1-C2	-167.4417	N28-C23-C24-N25	-0.4348
C5-C8-C9-C10	-131.8099	N28-C23-C24-C129	179.7691
C24-N25-C26-C27	0.3316	N22-C23-N28-C27	178.5698
N28-C27-C26-N25	0.0116	C24-C23-N28-C27	0.7528
C8-C9-C10-C11	-177.7803	C23-C24-N25-C26	-0.1246
C8-C9-C14-C13	177.445	C129-C24-N25-C26	179.6743
C10-C9-C14-C13	0.329	C23-N28-C127-C26	-0.5691

Table 2S. Experimental and theoretical wave numbers obtained for (FT-IR and Raman) spectral values of HDE

Mode Nos	IR	Raman	Unscaled	Scaled	I_{IR}	I_{Raman}	Vibrational Assignments with TED ≥ 10
1			17	16	2.47	15.79	$\tau C13 C12 C3 N10$ (40) + $\tau C1 C5 C2 C3$ (18) + $\tau C2 C1 N23 N24$ (11)
2			26	25	4.03	6.72	$\tau C1 C5 N10 C4$ (33) + $\tau C3 C2 N10 C4$ (10) + $\tau N23 N24 C26 N28$ (10)
3			28	27	2.1	10.19	$\tau C13 C12 C3 N10$ (32) + $\tau C2 C1 N23 N24$ (18)
4			30	29	1.62	15	$\tau C3 C2 N10 C4$ (11) + $\tau N23 N24 C26 N28$ (15) + $\tau C1 N23 N24 C26$ (16)
5			41	39	3.61	12.83	$\tau C1 N23 N24 C26$ (21)
6			45	43	2.25	12.15	$\beta C43 C4 N10$ (11) + $\tau C3 C2 N10 C4$ (13) + $\beta C12 C3 N10$ (11) + $\tau C1 N23 N24 C26$ (10)
7			50	48	2.01	15.54	$\tau C45 C43 C4 N10$ (43) + $\tau N23 N24 C26 N28$ (13)
8			75	72	4.55	5.16	$\tau C1 N23 N24 C26$ (14) + $r C12 C2 N10 C3$ (11) + $\beta C26 N24 N23$ (13)
9			88	84	3.97	6.28	$\tau N23 N24 C26 N28$ (10) + $\tau C1 C5 C2 C3$ (11) + $r C4 C43 C45 C44$ (10)
10			89	85	3.48	4.46	$\tau C4 C5 C35 C38$ (44)
11			118	113	10.26	7.2	$\tau C31 N29 C30 N28$ (21)
12			130	125	8.41	9.14	$\beta N24 C26 N28$ (11) + $\tau C31 N29 C30 N28$ (18)
13			144	138	0.98	4.3	$r C43 C5 N10 C4$ (12)
14			167	160	8.4	6.04	$\beta C1 C5 C35$ (32)

15			204	196	4.81	6.24	$\beta C5 C1 N23 (13) + \beta C3 C12 C13 (16)$
16			209	201	9.64	7.32	$rC35 C1 C4 C5 (15) + \beta N29 C27 C134 (11)$
17			236	227	10.33	13.58	$\tau C45 C48 C46 C50 (11)$
18			246	236	5.77	6.47	$\tau H39 C38 C35 C5 (17) + \beta C2 C3 N10 (10) + \tau H41 C38 C35 C5 (21)$
19			258	248	3.38	9.14	$\beta C4 C43 C45 (22)$
20			264	253	9.04	4.72	$\beta C3 C12 C13 (19) + \beta N29 C27 C134 (11)$
21			283	272	5.31	7.22	$\beta C5 C4 N10 (19) + vC4 C43 (12)$
22			290	278	16.45	7.6	$rC134 C26 N29 C27 (23) + \tau C26 N28 C31 C30 (10) + rN24 C26 N28 C27 (12)$
23			319	306	14.25	11.82	$\beta C26 N24 N23 (16) + \beta N24 C26 N28 (12)$
			338	324	1.43	4.33	$\beta C5 C35 C38 (22)$
25			369	354	10.12	5.15	$\beta C12 C3 N10 (10) + \beta N29 C27 C134 (10) + \tau C14 C17 C15 C19 (12)$
26			407	391	17.94	11.59	$vC134 C27 (32) + \beta C27 N29 C31 (19)$
27			415	398	5.98	5.65	$\tau C14 C17 C15 C19 (26) + \tau C15 C13 C19 C17 (31) + \tau C12 C14 C19 C17 (13) + \tau H20 C15 C13 C12 (11)$
28			418	401	24.12	14.69	$\beta N29 C27 C134 (14) + vC134 C27 (18)$
29			420	403	6.63	6.23	$\tau C46 C44 C50 C48 (27) + \tau C45 C48 C46 C50 (23) + \tau H47 C44 C46 C50 (10)$
30			429	412	11.76	7.69	$\beta C5 C35 C38 (16)$
31	459	456	473	454	20.7	7.79	$\beta C2 C1 C5 (11) + vC4 C5 (11)$

32	484	485	485	466	21.27	5.46	$r_{C134 C26 N29 C27}$ (25) + $\tau_{C26 N28 C31 C30}$ (11) + $\tau_{C30 C27 C31 N29}$ (11)
33	501	503	525	504	15.55	6.05	$r_{C4 C43 C45 C44}$ (14) + $r_{C3 C12 C13 C14}$ (15)
34			529	508	12.78	8.84	$\tau_{H25 N24 N23 C1}$ (10) + $v_{C26 C27}$ (13)
35			556	534	34.33	5.26	$\beta_{C2 C3 N10}$ (14)
36			567	544	22.8	4.1	$\tau_{C30 C27 C31 N29}$ (13) + $r_{N24 C26 N28 C27}$ (20)
37			572	549	25.78	5.58	$\beta_{C27 N29 C31}$ (13) + $\beta_{C45 C48 C50}$ (16)
38			597	573	19.79	13.6	$\beta_{C30 C31 N29}$ (28) + $\beta_{C31 C30 N28}$ (12)
39			615	590	70.4	7.23	$\tau_{H25 N24 N23 C1}$ (15)
40			626	601	50.77	11.46	$\beta_{C44 C46 C50}$ (13) + $\beta_{C45 C48 C50}$ (12)
41			634	609	6.59	10.78	$\beta_{C14 C17 C19}$ (24) + $\beta_{C13 C15 C19}$ (10) + $\beta_{C44 C46 C50}$ (15)
42			636	611	19.31	15.25	$\beta_{C14 C17 C19}$ (14) + $\beta_{C13 C15 C19}$ (12)
43			640	614	23.56	7.7	$\beta_{C45 C48 C50}$ (13) + $\beta_{C46 C50 C48}$ (32)
44			698	670	63.17	6.83	$v_{C134 C27}$ (10) + $\beta_{C27 N29 C31}$ (11)
45			716	687	41.82	7.35	$\tau_{C15 C13 C19 C17}$ (15) + $\tau_{C12 C14 C19 C17}$ (17) + $\tau_{H22 C19 C17 C14}$ (19)
46			718	689	39.28	5.79	$\tau_{C46 C44 C50 C48}$ (14) + $\tau_{C45 C48 C46 C50}$ (12) + $\tau_{H53 C50 C48 C45}$ (14) + $\tau_{H47 C44 C46 C50}$ (11)
47	697	693	733	704	26.99	15.51	$\tau_{H11 N10 C4 C5}$ (20) + $\beta_{H36 C35 C38}$ (11)
48			761	731	65.46	18.79	$\tau_{H52 C48 C50 C46}$ (24) + $\tau_{H53 C50 C48 C45}$ (25)
49			770	739	6.08	6.92	$\tau_{H36 C35 C5 C4}$ (24) + $\tau_{H41 C38 C35 C5}$ (13)

50			774	743	29.34	7.1	$\tau\text{C31 N29 C30 N28 (11) + } \tau\text{C26 N28 C31 C30 (24) + } \tau\text{C43 C45 C50 C48 (26) + } \tau\text{C30 C27 C31 N29 (17) + } \tau\text{N24 C26 N28 C27 (27)}$
51			780	749	36.7	10.18	$\tau\text{H21 C17 C19 C15 (12)}$
52	754	753	788	756	40.81	5.58	$\tau\text{H22 C19 C17 C14 (13) + } \tau\text{H20 C15 C13 C12 (16)}$
53			802	770	60.48	14.89	$\beta\text{C30 C31 N29 (12) + } \tau\text{H25 N24 N23 C1 (13)}$
54			826	793	62.12	11.43	$\tau\text{H11 N10 C4 C5 (17)}$
55			847	813	32.76	10.99	$\nu\text{C1 C2 (14) + } \nu\text{C1 C5 (21)}$
56			856	822	38.08	7.78	$\tau\text{H33 C31 N29 C27 (70) + } \tau\text{H32 C30 N28 C26 (24)}$
57			863	828	20.57	17.43	$\tau\text{H18 C14 C12 C3 (20) + } \tau\text{H49 C45 C48 C50 (20)}$
58			864	829	9.9	22.6	$\tau\text{H16 C13 C12 C3 (27) + } \tau\text{H20 C15 C13 C12 (21) + } \tau\text{H21 C17 C19 C15 (26) + } \tau\text{H51 C46 C50 C48 (21) + } \tau\text{H52 C48 C50 C46 (25) + } \tau\text{H47 C44 C46 C50 (28) +}$
59			876	841	16.19	14.49	$\nu\text{C4 C43 (10) + } \nu\text{C43 C45 (11)}$
60			911	875	50.55	17.38	$\tau\text{H25 N24 N23 C1 (10) + } \nu\text{N28 C26 (11)}$
61			927	890	29.37	15.68	$\tau\text{H49 C45 C48 C50 (10) + } \tau\text{H51 C46 C50 C48 (15)}$
62			934	897	7.91	7.71	$\tau\text{H16 C13 C12 C3 (23) + } \tau\text{H22 C19 C17 C14 (21) + } \tau\text{H18 C14 C12 C3 (18)}$
63			936	899	17.83	4.92	$\tau\text{H53 C50 C48 C45 (19) + } \tau\text{H47 C44 C46 C50 (17) + } \tau\text{H49 C45 C48 C50 (14)}$
64	920	920	961	923	5.65	2.98	$\tau\text{H33 C31 N29 C27 (22) + } \tau\text{H32 C30 N28 C26 (64)}$
65			966	927	25.95	12.16	$\nu\text{C2 C3 (19) + } \nu\text{N23 N24 (16)}$

66			976	937	12.08	5.17	$\tau\text{H47 C44 C46 C50 (14) + } \tau\text{H49 C45 C48 C50 (19) + } \tau\text{H51 C46 C50 C48 (23) + } \tau\text{H52 C48 C50 C46 (16)}$
67			977	938	7.56	1.88	$\tau\text{H16 C13 C12 C3 (17) + } \tau\text{H18 C14 C12 C3 (22) + } \tau\text{H20 C15 C13 C12 (18) + } \tau\text{H21 C17 C19 C15 (13)}$
68			980	941	23.72	8.35	$\tau\text{C12 C14 C19 C17 (13) + } \tau\text{C45 C48 C46 C50 (12)}$
69	949	951	987	948	32.44	15.27	$v\text{C4 C5 (22) + } v\text{N23 N24 (64)}$
70			999	959	19.3	23.01	$v\text{C30 C31 (11) + } v\text{N28 C30 (12)}$
71			1000	960	14.36	5.91	$\tau\text{H18 C14 C12 C3 (14) + } \tau\text{H20 C15 C13 C12 (13) + } \tau\text{H21 C17 C19 C15 (21) + } \tau\text{H22 C19 C17 C14 (19)}$
72			1016	975	8.54	38.16	$\beta\text{C14 C17 C19 (14) + } \beta\text{C15 C19 C17 (12) + } \beta\text{C13 C15 C19 (21)}$
73			1017	976	6.82	20.12	$\beta\text{C45 C48 C50 (19) + } \beta\text{C46 C50 C48 (13) + } \beta\text{C44 C46 C50 (22)}$
74			1023	982	14.55	7.86	$\beta\text{C1N23 N24 (31)}$
75			1053	1011	10.32	18.11	$v\text{C35 C38 (47) + } v\text{C5 C35 (17)}$
76			1059	1017	19.64	15.55	$v\text{C46 C50 (18) + } v\text{C48 C50 (18)}$
77			1061	1019	12.3	21.69	$v\text{C17 C19 (16) + } v\text{C15 C19 (19)}$
78			1067	1024	100	22.17	$v\text{C134 C27 (11) + } \beta\text{C31 C30 N28 (10) + } \beta\text{C27 N29 C31 (18)}$
79			1084	1041	29.46	18.8	$v\text{C5 C35 (11) + } \tau\text{H40 C38 C35 C5 (14) + } v\text{N10 C4 (13)}$
80			1096	1052	54.54	8.04	$v\text{N10 C3 (39) + } v\text{N10 C4 (34)}$
81			1106	1062	24.17	5.92	$v\text{C44 C46 (16) + } \beta\text{H53 C50 C48 (11) + } v\text{C45 C48 (13)}$

82	1114	1069	22.07	14.73	$vC13 C15 (15) + vC14 C17 (14) + \beta H22 C19 C17 (10)$
83	1122	1077	26	19.94	$\tau H39 C38 C35 C5 (12)$
84	1125	1080	63.37	23.64	$\beta H32 C30 N28 (16) + \beta H47 C44 C46 (10) + vC30 C31 (28)$
85	1157	1111	10.3	18.97	$\beta H47 C44 C46 (16) + vC45 C48 (10)$
86	1183	1136	35.25	12.09	$\beta H7 C2 C1 (34) + \tau H6 C2 C1 C5 (16)$
87	1187	1140	13.61	20.29	$\beta H52 C48 C50 (18) + \beta H53 C50 C48 (33)$
88	1188	1140	5.87	26.06	$\beta H20 C15 C13 (20) + \beta H21 C17 C19 (17) + \beta H22 C19 C17 (33) + \beta H51 C46 C50 (22)$
89	1213	1164	12.9	13.73	$\beta H51 C46 C50 (16) + \beta H52 C48 C50 (21) + \beta H49 C45 C48 (16)$
90	1214	1165	71.89	16.45	$vN29 C31 (35) + \beta H33 C31 N29 (17)$
91	1217	1168	16.4	16.6	$\beta H20 C15 C13 (13) + \beta H21 C17 C19 (22) + vC14 C17 (11) + \beta H16 C13 C12 (18) + \beta H18 C14 C12 (18)$
92	1225	1176	14.97	25.52	$vC4 C43 (25) + vC43 C44 (14)$
93	1229	1180	11.12	34.7	$vC3 C12 (16) + \beta H9 C3 N10 (21) + vC12 C13 (12)$
94	1258	1208	34.15	12.77	$vC1 C2 (10) + vC1 C5 (14)$
95	1264	1213	25.26	15.1	$\tau H8 C5 C1 C2 (14)$
96	1285	1234	25.16	14.53	$\beta H9 C3 N10 (12) + \tau H7 C2 C1 5C (18) + \tau H6 C2 C1 C5 (12)$
97	1289	1237	20.94	22.72	$\beta H33 C31 N29 (15) + vN28 C30 (24) + vN29 C27 (18)$
98	1300	1248	16.47	16.06	$\beta H8 C5 C1 (49)$

99			1313	1260	58.65	13.14	τ H6 C2 C1 C5 (13)
100			1334	1281	16.18	19.03	τ H36 C35 C5 C4 (11) + τ H37 C35 C5 C4 (24) + β H36 C35 C38 (16)
101	1287	1288	1343	1289	18.03	9.11	ν C12 C14 (10)
102			1349	1295	51.04	19.75	β H33 C31 N29 (10) + β H32 C30 N28 (29) + ν N28 C30 (11) + ν C26 C27 (10)
103			1357	1303	13.44	8.22	β H36 C35 C38 (10) + τ H8 C5 C1 C2 (14)
104			1364	1309	11.28	9.5	β H49 C45 C48 (15) + β H47 C44 C46 (13) + ν C45 C48 (14) + ν C44 C46 (13)
105			1369	1314	4.84	7.17	β H16 C13 C12 (21) + β H18 C14 C12 (27) + β H22 C19 C17 (10)
106			1380	1325	14.97	16.95	β H36 C35 C38 (11) + τ H8 C5 C1 C2 (11)
107			1383	1328	31.58	12.61	τ H42 C4 C43 C44 (15) + τ H37 C35 C5 C4 (11)
108			1395	1339	16.24	10.16	τ H9 C3 C12 C14 (26)
109			1405	1349	38.1	4.22	τ H42 C4 C43 C44 (16) + τ H9 C3 C12 C14 (24)
110			1406	1350	94.4	41.52	β H42 C4 N10 (20) + β H25 N24 N23 (12) + ν N29 C27 (10)
111			1430	1373	9.11	10.37	β H39 C38 H41 (37) + β H39 C38 H40 (27)
112	1411	1412	1489	1429	23.75	9.65	β H40 C38 H41 (29)
113			1490	1430	63.14	26.72	β H33 C31 N29 (24) + β H32 C30 N28 (15) + β H6 C2 H7 (42) + β H6 C2 H7 (10)
114			1494	1434	52.12	10.84	β H11 N10 C4 (28) + β H53 C50 C48 (10)

115			1497	1437	46.55	5.11	$\beta\text{H11 N10 C4 (21) + } \beta\text{H53 C50 C48 (10) + } \beta\text{H42 C4 N10 (11)}$
116			1498	1438	35.43	8.39	$\beta\text{H22 C19 C17 (14) + } \beta\text{H6 C2 H7 (13) + } \beta\text{H36 C35 H37 (14)}$
117			1501	1441	97.68	26.14	$v\text{N24 C26 (11) + } \beta\text{H25 N24 N23 (22) + } \beta\text{H36 C35 H37 (20)}$
118			1504	1444	81.78	27	$\beta\text{H25 N24 N23 (17) + } \beta\text{H6 C2 H7 (10) + } \beta\text{H36 C35 H37 (18)}$
119			1512	1452	24.59	22.02	$\beta\text{H39 C38 H41 (41) + } \tau\text{H41 C38 C35 C5 (14) + } \beta\text{H40 C38 H41 (30)}$
120	1459	1459	1518	1457	26.61	9.23	$\beta\text{H36 C35 H37 (19) + } \beta\text{H39 C38 H40 (39) + } \beta\text{H40 C38 H41 (19) + } \tau\text{H40 C38 C35 C5 (11)}$
121			1541	1479	27	4.98	$\beta\text{H49 C45 C48 (14) + } \beta\text{H51 C46 C50 (14) + } \beta\text{H52 C48 C50 (14) + } \beta\text{H47 C44 C46 (12) + } v\text{C46 C50 (10) + } v\text{C48 C50 (10)}$
122			1543	1481	28.42	7.72	$\beta\text{H16 C13 C12 (13) + } \beta\text{H18 C14 C12 (17) + } \beta\text{H20 C15 C13 (18) + } \beta\text{H21 C17 C19 (16)}$
123			1573	1510	76.76	36.56	$v\text{N28 C26 (36) + } v\text{N29 C31 (10) + } v\text{N29 C27 (10) + } v\text{C30 C31 (12)}$
124	1534	1534	1618	1553	84.57	27.16	$v\text{N29 C27 (22) + } v\text{C30 C31 (15) + } v\text{N28 C30 (16) + } v\text{C26 C27 (15)}$
125			1640	1574	37.19	34.28	$v\text{C48 C50 (13) + } v\text{C46 C50 (11) + } v\text{C48 C50 (10)}$
126			1641	1575	15.83	33.11	$v\text{C15 C19 (12) + } v\text{C12 C13 (10) + } v\text{C43 C45 (10)}$
127			1662	1596	16.24	35.32	$v\text{C45 C48 (20) + } v\text{C44 C46 (20) + } v\text{C43 C45 (10) + } v\text{C43 C44 (12)}$

128	1602	1601	1663	1596	15.02	36.09	vC14 C17 (22) + vC13 C15 (22) + vC12 C13 (10)
129	1719	1716	1716	1647	75.49	28.35	vN23 C1 (79)
130			3021	2900	30.35	20.73	vC4 H42 (95)
131			3022	2901	51.17	36.1	vC3 H9 (88) + vC2 H7 (10)
132			3029	2908	43.37	42.17	vC35 H36 (74) + vC35 H37 (20)
133			3049	2927	58.55	86.02	vC2 H7 (76)
134	2932	2934	3050	2928	43.62	46.12	vC38 H40 (18) + vC38 H41 (38) + vC38 H39 (37)
135			3072	2949	37.13	43.91	vC35 H36 (20) + vC35 H37 (75)
136	2970	2970	3115	2990	49.01	52.39	vC38 H41 (50) + vC38 H39 (46)
137			3126	3001	35.73	29.1	vC5 H8 (94)
138			3136	3011	45.32	28.77	vC38 H39 (13) + vC38 H40 (75)
139			3142	3016	29.33	46.46	vC2 H6 (92)
140			3172	3045	22.57	27.53	vC44 H47 (62) + vC46 H51 (24)
141			3175	3048	13.46	28.48	vC13 H16 (33) + vC15 H20 (33) + vC17 H21 (12) + vC19 H22 (21)
142			3179	3052	4.08	52.54	vC44 H47 (17) + vC50 H53 (20) + vC45 H49 (15) + vC48 H52 (48)
143			3182	3055	16.64	59.64	vC13 H16 (34) + vC17 H21 (39) + vC19 H22 (17)
144			3184	3057	22.21	42.6	vC31 H33 (12) + vC30 H32 (88)
145			3189	3061	36.87	63.25	vC44 H47 (14) + vC50 H53 (25) + vC45 H49 (21) + vC46 H51 (30) + vC48 H52 (10)

146			3191	3063	45.44	52.62	vC13 H16 (23) + vC17 H21 (23) + vC14 H18 (11) + vC15 H20 (24) + vC19 H22 (18)
147			3197	3069	42.74	15.55	vC45 H49 (50) + vC46 H51 (25) + vC48 H52 (13)
148			3201	3073	38.32	37.33	vC14 H18 (43) + vC15 H20 (28) + vC19 H22 (21)
149			3206	3078	41.49	99.28	vC45 H49 (12) + vC46 H51 (20) + vC48 H52 (24) + vC50 H53 (40)
150			3207	3079	36.93	100	vC14 H18 (38) + vC15 H20 (11) + vC17 H21 (25) + vC19 H22 (22)
151	3102	3103	3212	3084	40.61	79.6	vC31 H33 (88) + vC30 H32 (12)
152			3497	3357	13.73	32.16	vN10 H11 (100)
153	3414	3412	3576	3433	63.76	52.86	vN24 H25 (100)

v - stretching, β - inplane bending, τ - torsional vibrations, γ - out of plane bending

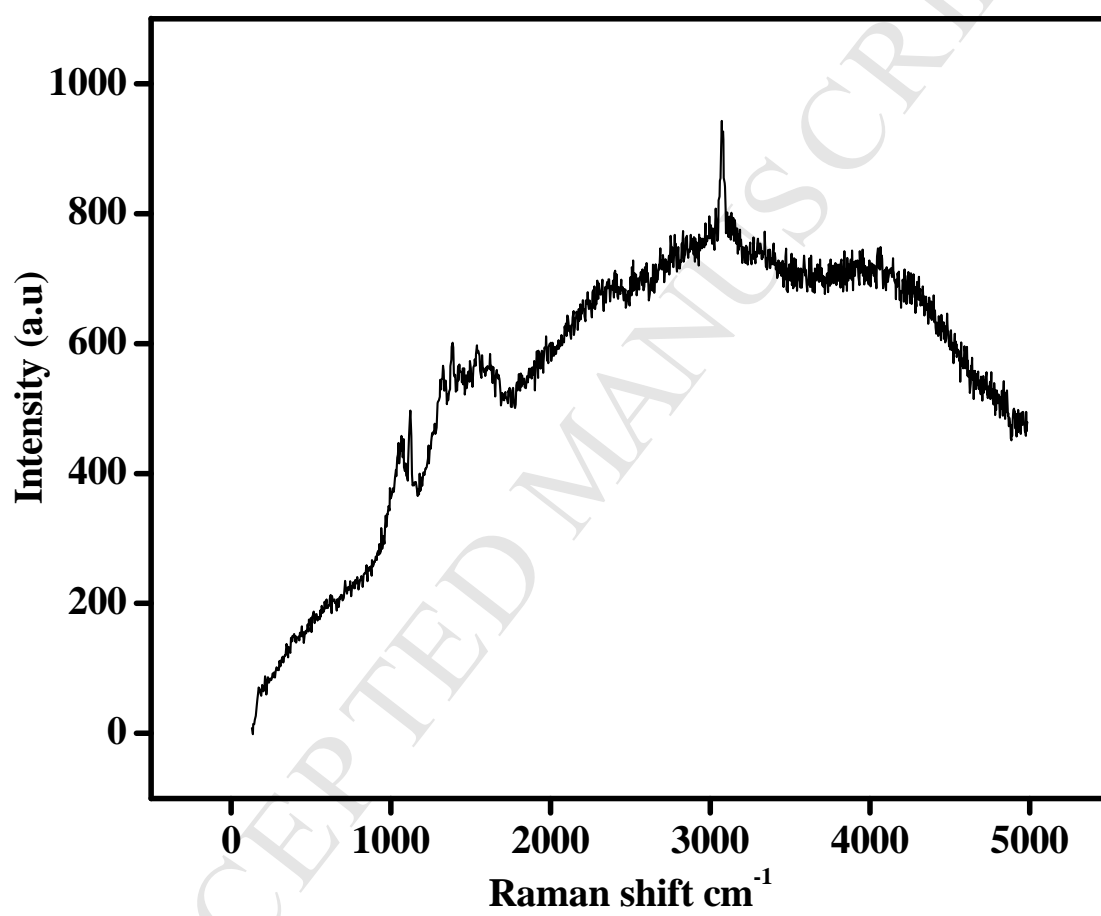


Figure 1S. Experimental Raman spectrum of HDE.

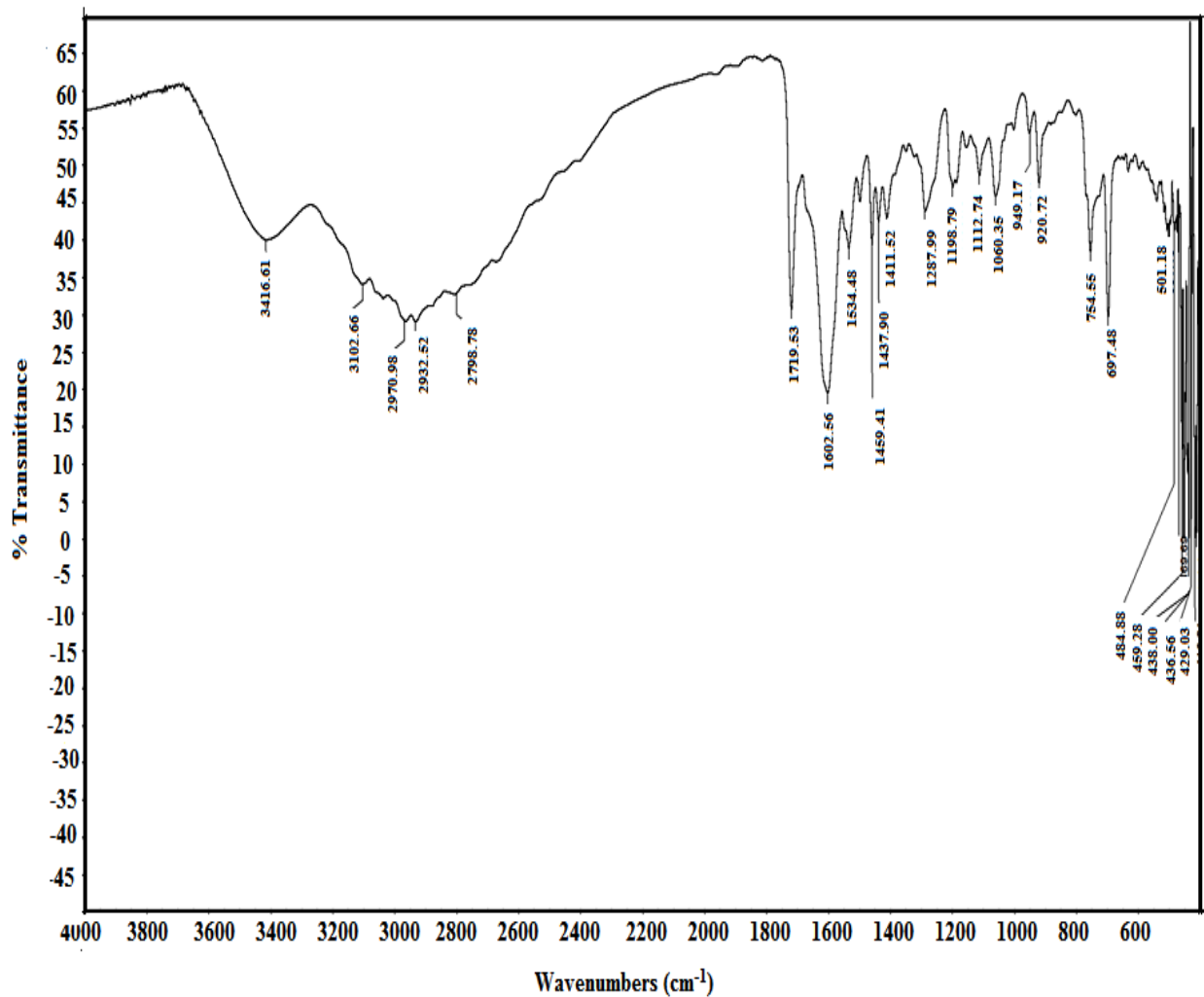


Figure 1S. Experimental IR spectrum of HDE.

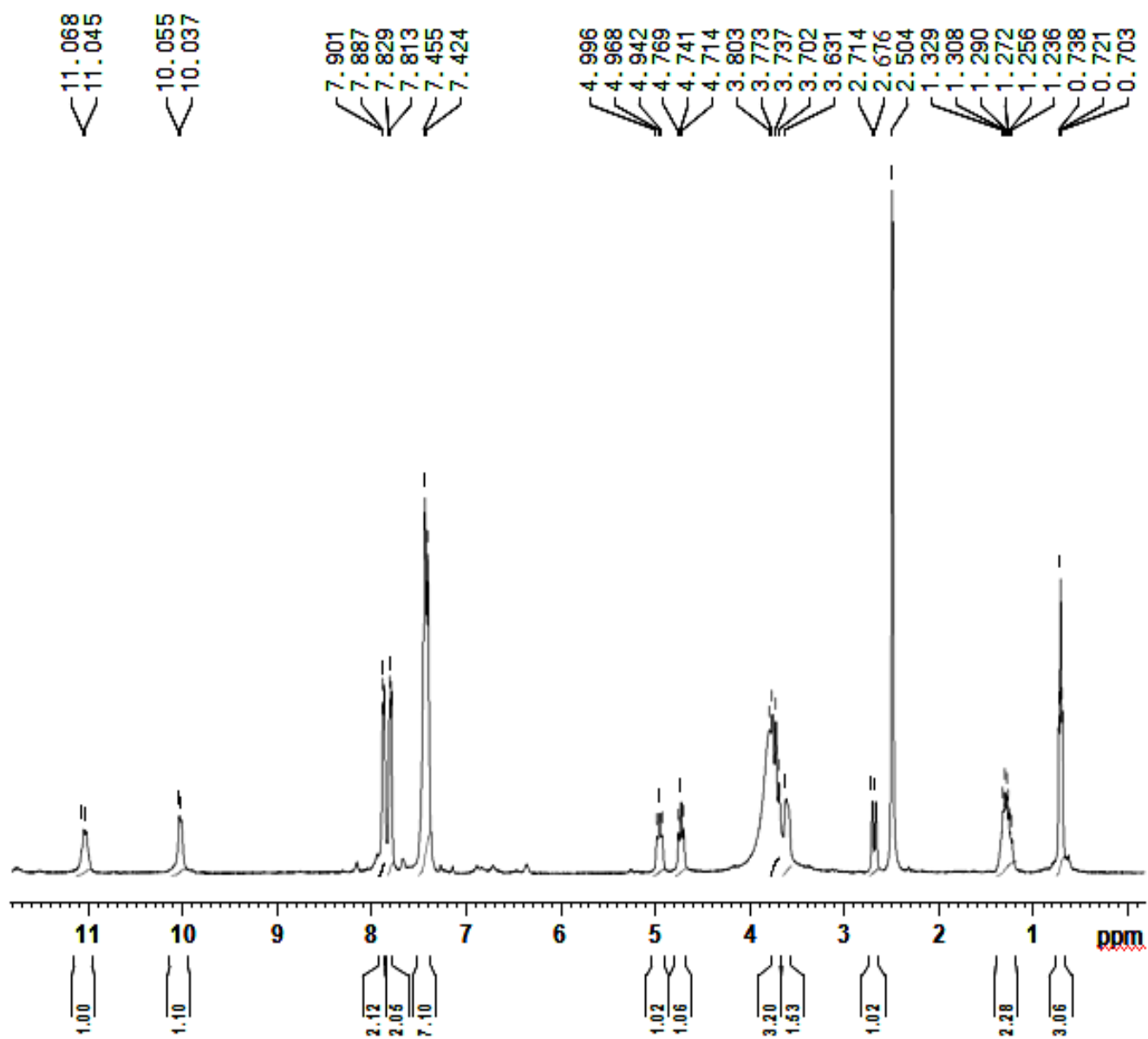


Figure 2S. Experimental ^1H NMR spectrum of HDE.

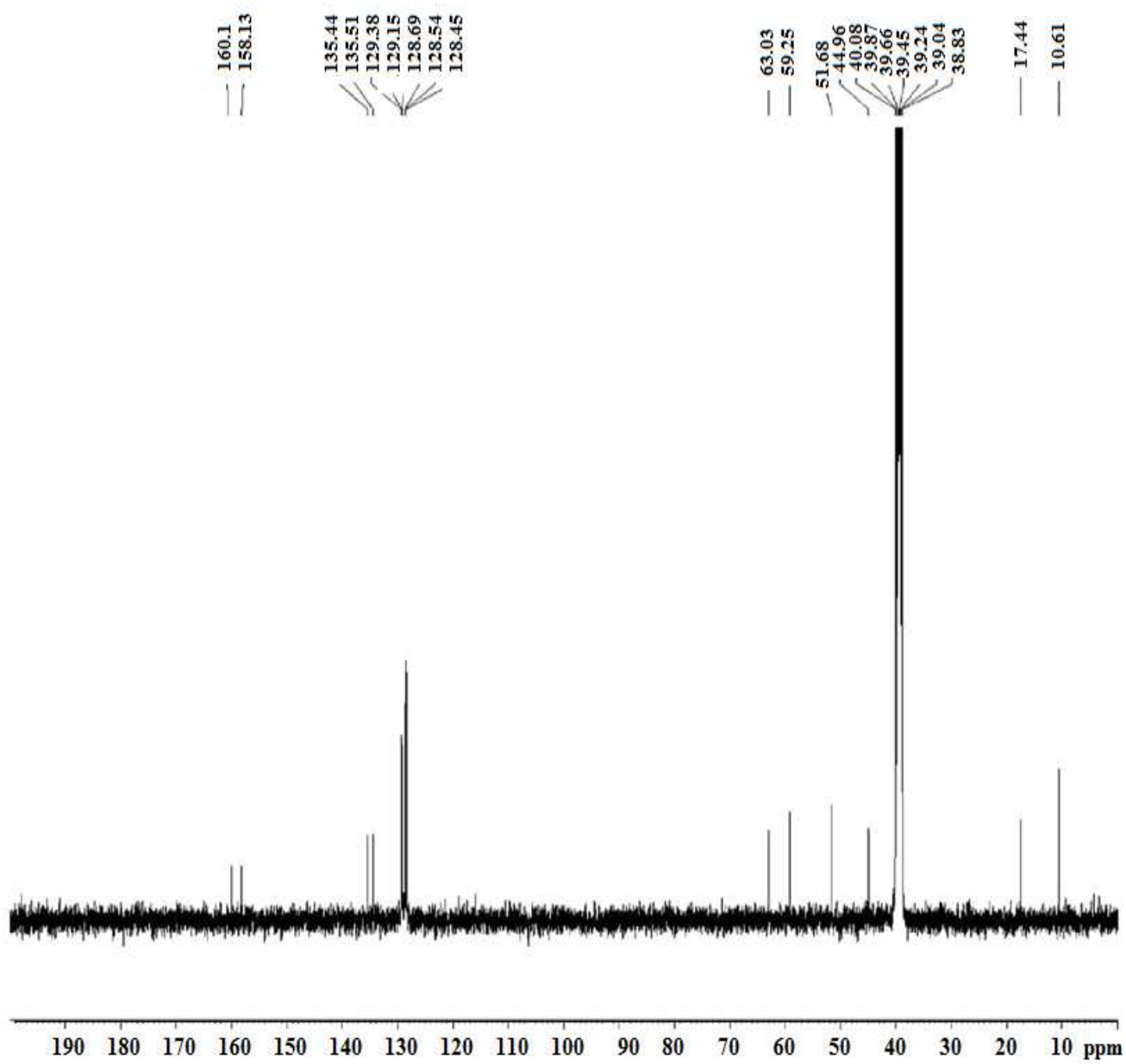


Figure 3S. Experimental ^{13}C NMR spectrum of HDE.

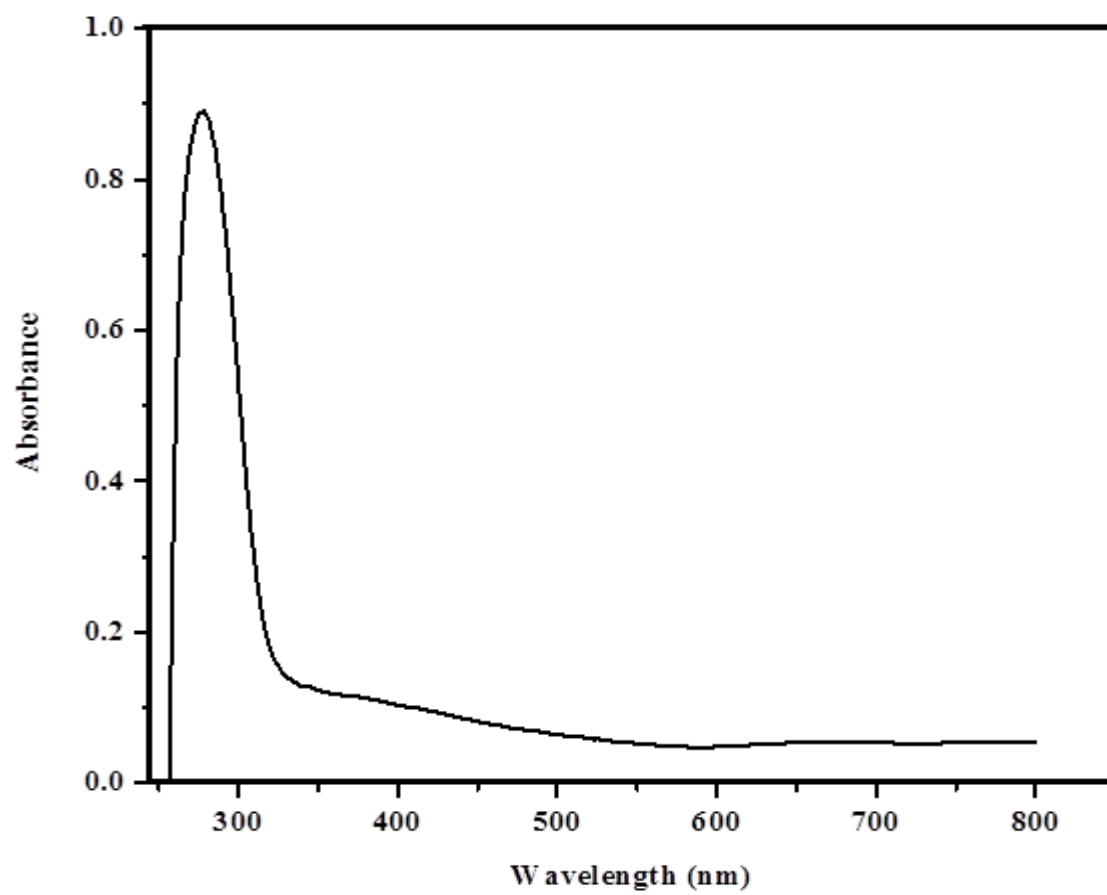


Figure 4S. UV spectrum of HDE.